Optical spectroscopy of field-induced charge in self-organized high mobility poly(3-hexylthiophene)

Peter J. Brown and Henning Sirringhaus*
Optoelectronics Group, Cavendish Laboratory, Madingley Road, Cambridge CB3 OHE, United Kingdom

Mark Harrison
Institute of Physical Chemistry and Department of Physics, Philipps-University of Marburg, D-35032 Marburg, Germany

Maxim Shkunov and Richard H. Friend
Optoelectronics Group, Cavendish Laboratory, Madingley Road, Cambridge CB3 OHE, United Kingdom
(Received 9 November 1999; revised manuscript received 20 November 2000; published 12 March 2001)

Charge modulation spectroscopy (CMS) is an electro-optical spectroscopic technique that allows the charge carriers present in the conducting channels of field-effect transistors (FET's) to be studied *in situ*. We use this technique to study the charge carriers present in regio-regular poly(3-hexylthiophene) P3HT that has been shown to exhibit high field-effect mobilities of up to 0.1 cm^2/Vs, similar to that observed for amorphous silicon. We demonstrate that the CMS spectra of charge carriers in high-mobility regio-regular P3HT FET's are independent of charge density, modulation frequency, and temperature. This is evidence for the presence of a single, intrinsic charge carrier that we identify as a singly charged polaronic species. The spectral features attributed to the charged species show a lack of vibronic structure that is in contrast to the vibronic structure present in the bleaching of the main π-π^* absorption of the neutral chains. The transition energies observed in regio-regular P3HT cannot be understood as an extrapolation of charge-induced transitions in isolated short-chain oligomers to long conjugation lengths. Our results give evidence that interchain coupling in highly ordered P3HT is sufficiently strong so that the charge carriers cannot be considered to be confined to a single chain, rather, they now exhibit quasi-two-dimensional characteristics.

DOI: 10.1103/PhysRevB.63.125204 PACS number(s): 71.20.Rv, 85.30.Tv

I. INTRODUCTION

In regio-regular, substituted poly(3-hexylthiophene) (P3HT) FET's a direct correlation between the high field-effect mobility (up to 0.1 cm^2/Vs) and the microcrystalline microstructure has been observed.[1,2] This has been brought about by improvements in the synthesis of the polymer such that the coupling of the asymmetric alkyl-thiophene rings gives rise to a high ratio of 2, 5′, or so-called Head-to-Tail, coupling between adjacent rings[3] (shown in Fig. 1). As a result of this high degree of intrachain order, the polymer chains self-order to form microcrystalline regions of π stacked lamella with strong interchain interactions.[4] Compared with disordered amorphous polythiophene, with mobilities less than 10^4 cm^2/Vs (Ref. 5), the high field-effect mobilities in regio-regular P3HT (that are comparable to those of α-Si) suggest that a new description of the charge carriers and the charge transport physics may be required.

The introduction of charge carriers onto an isolated conjugated molecule is accompanied with a polaronic structural and electronic relaxation of the conjugated backbone. Singly charged carriers are referred to as polarons (or radical cations in the case of short oligomers) whereas doubly charged carriers are called bipolarons (dications). This relaxation results in the appearance of new optical transitions in the absorption spectrum at energies beneath the main π-π transition upon charge injection. These transitions have been detected experimentally[6–14] and are in good agreement[15] with the quantum chemical calculations of Cornil *et al.*[16–19] performed on isolated oligomers (see Fig. 2) and earlier tight-binding models of isolated, one-dimensional polymer chains developed by Su, Schrieffer, and Heeger (the SSH model) (Ref. 20) and Fesser, Bishop, and Campbell (the FBC model).[21] These experiments suggest that polymer chains may be regarded as a sequence of short, isolated, oligomeric segments separated by disorder-induced conjugation defects. In this picture, the charge carriers are confined to the short conjugated segments and exhibit a pronounced oligomeric character.[22]

Several groups have attempted to remove the limitation of modeling only isolated chains by including the effects of interchain interactions in conjugated materials.[23–26] They showed that the one-dimensional nature of the charge carriers is stabilized by disorder, preventing the charge carriers

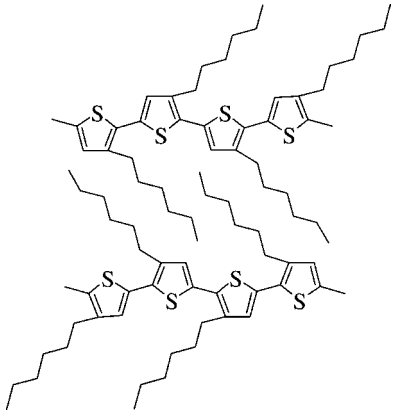

FIG. 1. Structure of regio-regular head-to-tail coupled poly (3-hexylthiophene).

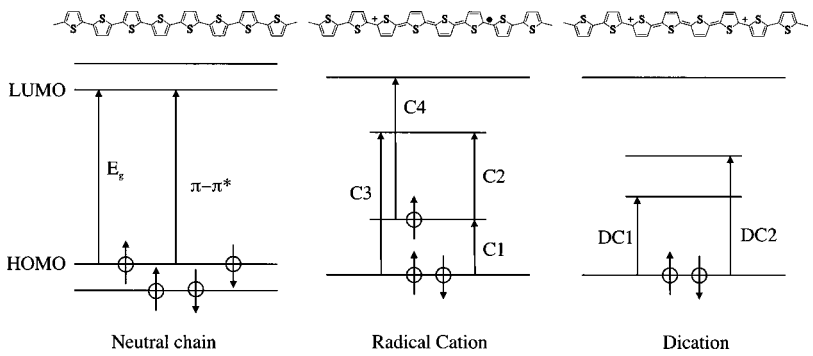

FIG. 2. The molecular energy levels of a 1D thiophene chain for neutral, singly, and doubly charged species along with the structure of the chain segments associated with each species. These results are similar to those obtained from the single-electron FBC model where a conduction band replaces the highest occupied molecular orbital level and a valence band replaces the lowest unoccupied molecular orbital level. The charged species would then be polarons and bipolarons with the levels labeled P1-4 and BP1-2, to avoid confusion between the models. Note that transitions C3, C4, and DC2 are usually disallowed due to symmetry considerations in isolated chains.

from spreading over neighboring chains. This is consistent with experimental observations that polarons in disordered polymer films in the solid state have a spectroscopic signature that is similar to isolated chains in solution,[27] implying that disorder tends to localize charge carriers onto individual chains.

A powerful experimental technique with which to directly probe charge carriers present in the conducting layer of FET's using injected charge, without isolating the chains in solution or introducing the presence of perturbing counter ions is charge modulation spectroscopy (CMS). The experiment modulates the charge density in a thin semiconducting film by modulating the applied gate bias in a semitransparent metal-insulator-semiconductor (MIS) diode device structure. By measuring the associated change in transmission, the characteristic spectroscopic signature of the field-induced charge can be detected.

Ziemelis *et al.*[28] performed CMS on thin films of regio-random P3HT and assigned the features observed to those of polarons and bipolarons predicted by the one-dimensional (1D) FBC model. Exhaustive CMS experiments on polycrystalline *nT* were performed by Harrison *et al.*[29–31] and these show that an equilibrium exists between polarons and bipolarons that is dependent on temperature, applied bias, and modulation frequency. Harrison *et al.* also observed evidence for weak interchain interactions in $6T$ in that transitions attributed to a transverse bipolaron, or π dimer, were observed.

These are important results as they show that even though interchain interactions should be important in the solid state, the chains could still be largely considered as isolated and quasi-one-dimensional. For regio-random P3HT this may be due to disorder in the film, however, in polycrystalline *nT* this may be an intrinsic effect related to the finite chain length of the molecule. It should also be noted that the fact that several different species are observed simultaneously suggests that the intrinsic charge carriers are not being observed and that a certain degree of disorder is stabilizing other species.

It is a point of great interest as to the nature of the charge carriers present in high-mobility regio-regular P3HT FET's. Here, we use CMS to fully characterize the charge carriers present in highly ordered regio-regular films of P3HT and offer an explanation for the improved FET performance and spectra observed in terms of the increase of the dimensionality of the conducting species.

II. EXPERIMENT

Figure 3 shows a schematic diagram of the MIS diodes used in this experiment. The configuration is very similar to that of FET devices allowing a direct comparison between field-effect charge transport and spectroscopic properties. To fabricate the MIS diodes, a semitransparent aluminum gate electrode was evaporated onto a glass substrate, on top of which a 130–150 nm thick layer of the insulator silicon dioxide was deposited by plasma enhanced chemical vapor deposition. The insulator was then treated with hexamethyldisilazane (HMDS) in order to replace the natural surface OH groups with hydrophobic methyl groups, as it is thought that this promotes structural ordering of the polymer at the interface. A layer of P3HT with a thickness of ~50 nm was spin coated onto the insulator, and a semitransparent ohmic gold electrode evaporated onto the polymer completed the device. This device structure can be compared with a parallel plate capacitor where a semiconductor has replaced the top plate.

The capacitance of our devices was measured as a function of applied bias and modulation frequency using a

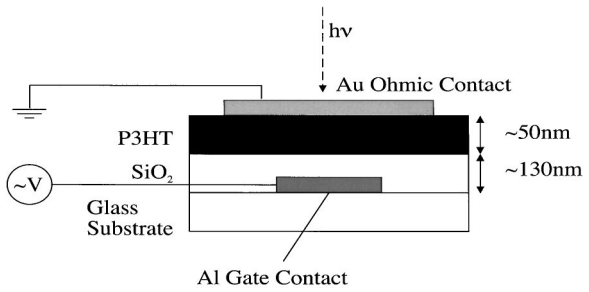

FIG. 3. Schematic diagram of an MIS diode with experimental setup for charge modulation spectroscopy.

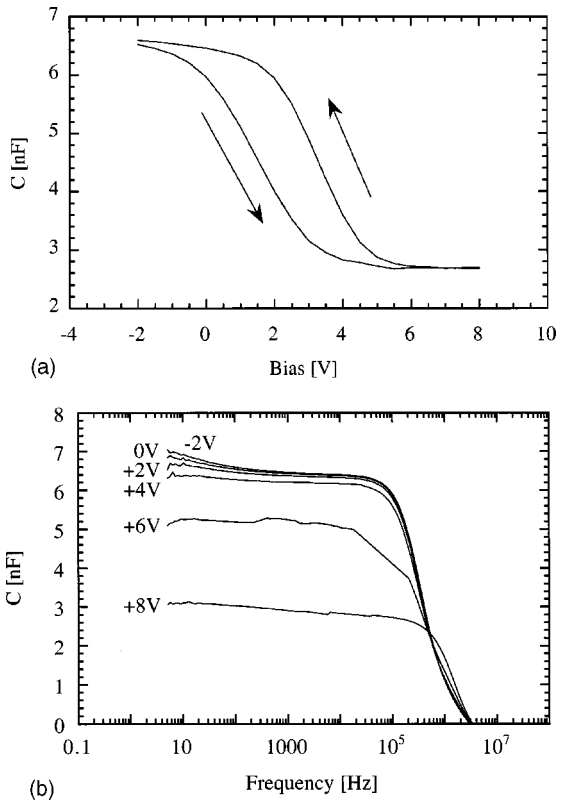

FIG. 4. (a) $C(V)$ and (b) $C(F)$ plots for the MIS diodes used in these experiments. The $C(V)$ scan was taken with a modulation frequency of 37 Hz.

Hewlett Packard 4192A LF Impedance Analyzer. Figure 4 shows the capacitance characteristics for the MIS diodes used in our experiments as a function of frequency and voltage [$C(F)$ and $C(V)$, respectively], exhibiting the expected increase of capacitance as the device is biased from depletion into accumulation.[32] From the $C(V)$ characteristics in accumulation at -2 V, corresponding to an electric field strength of about 200 kV/cm across the insulator, the sheet charge-carrier density in the accumulation layer is estimated to be on the order of $10^{18}\,\mathrm{cm}^{-3}$ (N.B., the dopant charge density, is ca. $1\times10^{17}\,\mathrm{cm}^{-3}$ in our P3HT devices). From the dimensions of the P3HT unit cell[33] we estimate that this corresponds to a charge density in the accumulation layer of approximately one charge every 1000 thiophene rings. This is low compared to the charge densities typically found in chemical doping experiments of about one charge per oligomeric molecule.

The technique of modulation spectroscopy has been used previously to study inorganic materials and, more recently, to study organic materials and is outlined in detail elsewhere.[30,34] Essentially, by applying a small ac bias to the gate electrode, typically ±1 Vac, the amount of charge stored in the device can be modulated resulting in a corresponding modulation of the transmittance of the incident monochromatic light (0.5 to 3.0 eV). This is detected using lock-in techniques. The spectrum obtained can be conceptually imagined as a difference spectrum between the device biased at V$+\delta$V and V$-\delta$V.

In the mid-IR range (ca. 0.1 to 0.5 eV) CMS spectra are obtained using a modified experimental technique. The device used for this experiment was an FET that was constructed on a lightly doped silicon substrate that formed the gate with a 200 nm thick SiO_2 gate insulator treated with HMDS. P3HT was deposited by spin-coating, and an evaporated gold source and drain electrodes completed the device. The characteristics of the FET's prepared for CMS experiments were comparable with those of standard FET devices with field-effect mobilities greater than $10^{-2}\,\mathrm{cm}^2/\mathrm{Vs}$. To extract the mid-IR CMS spectrum of this device Fourier transform infrared (FTIR) absorption spectra were measured with the device biased at $+5$ and -30 V, taking typically ca. 20,000 averages. The difference spectrum of the $+5$ V spectrum subtracted from the -30 V spectrum gave the CMS spectrum.

When the MIS devices are biased into accumulation, the spectrum of the charge carriers present in the conducting channel of FET devices is obtained. As the applied ac bias modulates the density of charge carriers present in the conducting channel, the absorption features of the subgap optical transitions (Fig. 2) are modulated, which shows up as features beneath the π-π^* transition in the spectra obtained. When the device is biased into depletion, the charge carriers present at the interface between the depletion layer and the bulk semiconductor are probed. When the device is biased into full depletion, then the experiment is essentially an electroabsorption experiment.

Electroabsorption occurs when the mobile charge carriers in the polymer cannot fully screen the core molecular electrons from the applied modulating field. When this happens, the energy levels in the polymer are modulated resulting in Stark shifts of the optical transitions. The line shape of the electroabsorption spectrum can be fitted to a linear sum of the absorption, the first derivative of the absorption spectrum with respect to the photon energy and the second derivative of the absorption. These effects are due to the Quadratic Stark Effect and the second-order Linear Stark Effect, respectively.[35]

Electroabsorption spectra were also measured in a surface cell geometry, consisting of a Herasil quartz substrate with interdigitated chrome electrodes of 160 μm spacing, onto which a 24 nm film of regio-regular P3HT was deposited by drop casting. An rms field strength of 70.7 kV/cm was applied. In contrast to CMS in depletion, this geometry allows the electroabsorption spectrum to be measured without any contribution from a bleaching signal, since essentially no charge is induced in the surface cell geometry.

III. RESULTS

The $C(V)$ and $C(F)$ characteristics of a typical P3HT MIS diode are presented in Fig. 4. These plots demonstrate that the devices operate as expected with a threshold voltage of ca. $+3$V, consistent with the low turn-on voltages for FET devices.[36] The hysteresis observed in the $C(V)$ characteristics, that are also present in the FET characteristics, are probably caused either by the slow trapping (relaxation) of the induced charge or by the migration of low-mobility dopant

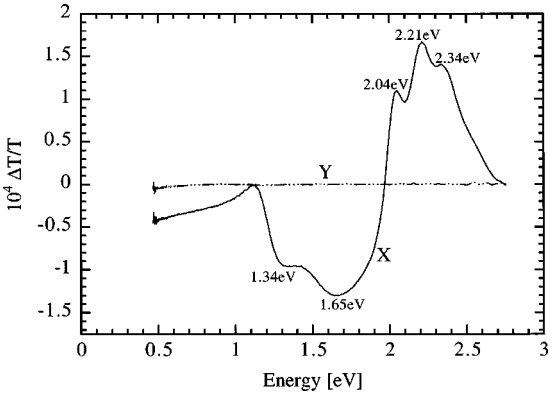

FIG. 5. CMS spectrum of P3HT biased into accumulation at room temperature. The applied dc bias was $0\ \mathrm{V} \pm 1\ \mathrm{V}$ ac with a modulation frequency of 37 Hz. The solid line corresponds to the in-phase (X) output of the lock-in amplifier, the dashed line to the quadrature (Y) output.

ions towards the accumulation layer.[37] The $C(F)$ spectrum shown in Fig. 4(b) is interesting as it demonstrates that the charges in the polymer continue to react to the applied modulating field faster than frequencies of ca. 100 kHz. This speed is comparable to those reported for the fastest oligomers[37] and is ca. 10–100 times faster than previously measured for low-mobility P3HT.[28] Above 100 kHz the measured capacitance of the device falls to 0 nF due to the contact resistance to the electrodes limiting charge injection into the device.

The CMS spectrum of a P3HT MIS diode taken in accumulation at $0\ \mathrm{V} \pm 1\ \mathrm{V}$ ac at room temperature and with a modulation frequency of 37 Hz is shown in Fig. 5. The features characterized by $\Delta T/T < 0$ are charge modulation features associated with the charge carriers present in the accumulation layer. The experiment yields both the in-phase (X) and quadrature (Y) signals and it is a feature of the spectra measured for P3HT that a unique phase can be selected such that Y can be set to zero for all charge modulation features. In general, this representation of the data allows a change of phase between different features to show up as a nonzero Y component in the signal. This is in direct contrast to the results obtained for nT which show a variation of phase for different resolvable charged features. The implications of this are discussed later. In Fig. 5, a main peak is seen at 1.65 eV and a shoulder is observed at ca. 1.34 eV. Between 1.2 and 0.5 eV $\Delta T/T$ rises to the edge of the detectable spectral range, indicating that there is at least one further subgap feature, at an energy less than 0.5 eV.

The region of the spectrum at energies greater than 1.97 eV, where $\Delta T/T > 0$, shows the bleaching of the main absorption feature of the π-π^* transition. This increase in transmission is due to the removal of neutral segments from the conjugated backbone and the associated π-π^* optical transition upon charging. The bleaching signal shows a structure with features at 2.04, 2.21, and 2.34 eV, whereas the charged features are smooth and structureless. These bleaching features correlate well with the vibronic structure observed in the absorption spectrum of the neutral polymer, as shown in Fig. 6. Here the X component of the CMS signal

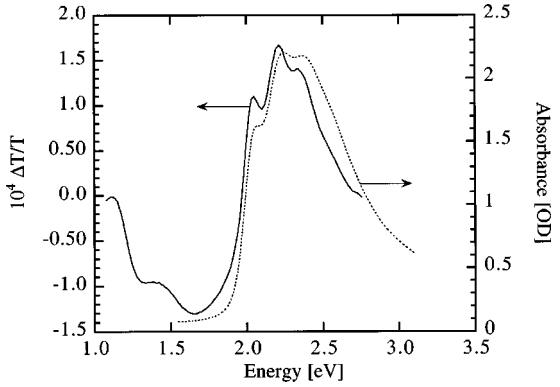

FIG. 6. The X component of Fig. 5 in comparison with the normal thin film absorption spectrum of P3HT emphasizing the similarity between the two spectra above 2.0 eV.

(initially shown in Fig. 5) is plotted together with the normal absorption spectrum of a thin P3HT film on a glass substrate. Close examination of Fig. 6 reveals that above 2.0 eV the CMS features are slightly redshifted and better resolved than their absorption spectrum counterparts.

To obtain further information about the nature of the charged excitations, we have taken spectra as a function of frequency, temperature, and applied bias. Previous CMS experiments on oligothiophenes and regio-random P3HT have shown that an equilibrium exists between polarons, bipolarons, and π-dimers that is dependent on applied bias and temperature.[28,31,38] Features due to different physical species are expected to have different characteristic responses to the modulation frequency and temperature, such that it should be possible to obtain a spectrum whereby different features have different phases.

Figure 7 shows how the spectrum shown in Fig. 5 evolves with increasing frequency. It can be seen that the relative phases or intensities of the features do not change even up to frequencies of 10 kHz.

Figure 8(a) shows the temperature dependence of the spectrum taken in accumulation with a modulation frequency of 37 Hz for a similar device. Note that the energies and intensities of the subgap features in Fig. 8 are not the same as shown in Figs. 5 and 6; this is because the exact appearance of the subgap features depends to some extent upon device

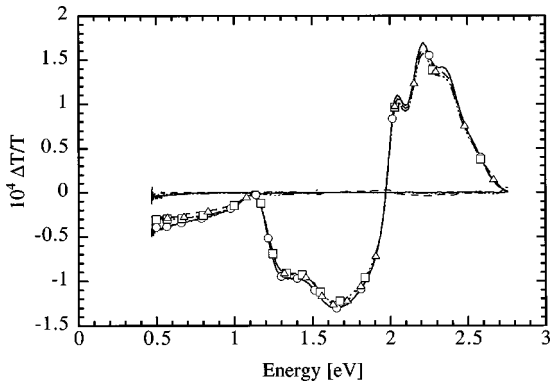

FIG. 7. Frequency dependence of the CMS spectrum of a P3HT device (37 Hz, circles; 1 kHz, squares; 10 kHz triangles).

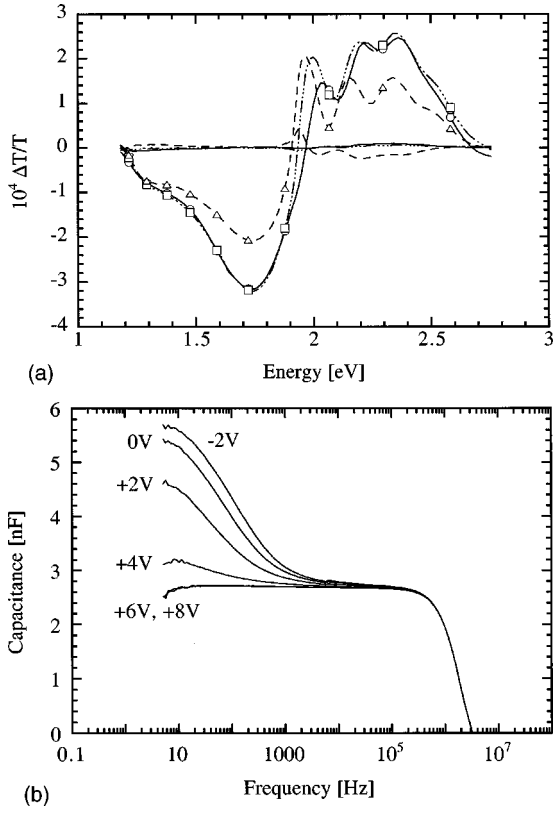

FIG. 8. (a) Temperature dependence of accumulation CMS spectrum at 37 Hz (room temperature, circles; 200 K, squares; 110 K triangles). (b) CF spectra of the device at 110 K at a range of biases from accumulation through to depletion.

preparation. In this device, the higher energy subgap feature is observed at 1.74 eV, however it is not possible to resolve whether the feature observed at 1.34 eV in Fig. 5 has shifted or not. Importantly, the behavior of the charge-induced, subgap features, with respect to modulation frequency, applied bias, or temperature is independent of device preparation. The main result to note in Fig. 8 is that the functional form of the features beneath the π-π^* transition is independent of temperature, although the features are slightly better resolved at lower temperatures. It is interesting to note that as the temperature decreases, the spectrum above 1.9 eV evolves from a bleaching response into a spectrum with a strong contribution from the electroabsorption signal (see discussion below). This is due to the reduction of the thermally activated mobility of the charge carriers that screen the applied modulating field. This reduction in mobility is also the cause of the reduction of the intensity of the subgap features and can also be inferred from the $C(F)$ spectrum, taken at 110 K and shown in Fig. 8(b). $\Delta T/T$ is proportional to the capacitance of the device and, hence, the reduction of the maximum capacitance at low frequency and of the roll-off frequency $\sim$10 Hz is consistent with the behavior seen above.

The data presented so far has been confined to the special case of the device biased into accumulation. Figure 9 shows how the CMS spectrum evolves as a P3HT device is biased from accumulation to full depletion. It should be noted that it

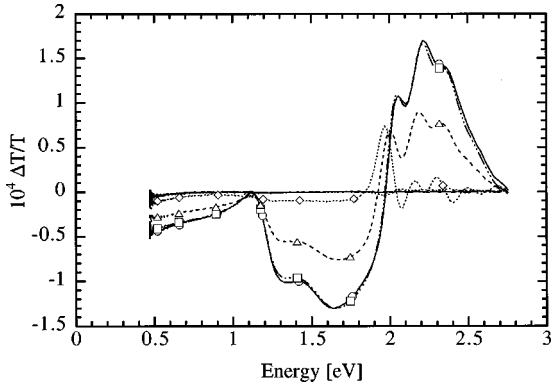

FIG. 9. Bias dependence of the CMS spectrum shown in Fig. 5 at room temperature (-5 V, circles, 0 V squares, $+5$ V triangles, $+10$ V diamonds).

was not possible to observe the device operating in full depletion until a $+10$ V bias was applied to the device. This is contrary to the $C(V)$ data presented in Fig. 4(a), where this regime was reached at a bias of $\sim+6$ V. This was because when the dc bias was applied for long periods of time, a shift of the threshold voltage to more positive values was observed; this is the same effect that resulted in the hysteresis of the $C(V)$ scans, as discussed earlier. The overall intensity of the subgap features decreases as the device is biased towards full depletion. At $+10$ V, the device is biased into full depletion and an electroabsorption signal, characterized by a feature at 1.95 eV, becomes significant.

The electroabsorption signal can also be seen in Fig. 10, which shows a CMS spectrum taken at 110 K in full depletion. As a direct comparison, an electroabsorption spectrum measured at 77 K in a surface cell geometry with interdigitated electrodes is also shown. Note that even when the device is fully depleted of mobile charge carriers, both at room temperature and 110 K, we still observe weak subgap transitions. It is possible that this is due to the presence of a leakage current through the gate insulator.

We suggested above that the pronounced fine structure of the bleaching signal is of vibronic origin. This would suggest that the charge carriers observed in the spectra are located in the most ordered domains of the film. However, to prove that

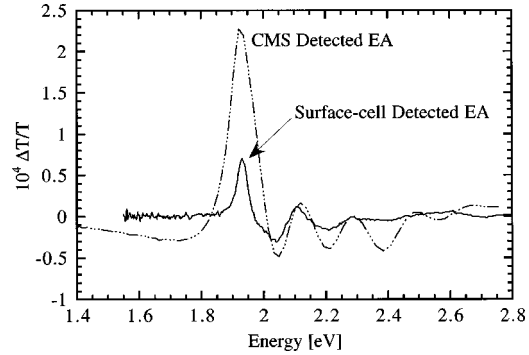

FIG. 10. CMS spectrum of a fully depleted device ($+7.5$ V ± 1 V ac) at 110 K that shows a dominant electroabsorption signal. The signal plotted in comparison is a pure electroabsorption signal measured in a surface cell geometry at a similar temperature.

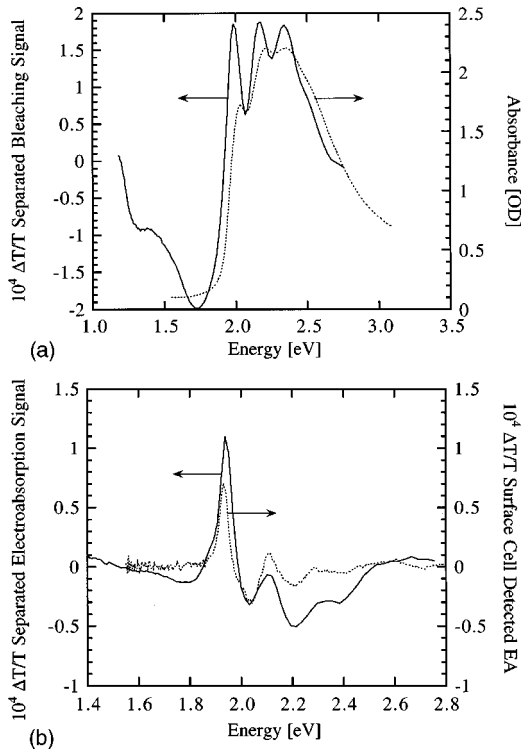

FIG. 11. Phase separated signals from the CMS spectrum obtained at 110 K, −2 V (see Fig. 8). (a) The bleaching signal, at a phase of +1°, plotted with the absorption spectrum of P3HT taken at a similar temperature. (b) The electroabsorption signal, at a phase of +26°, plotted with the pure electroabsorption signal obtained in the surface cell geometry (see Fig. 9).

the fine structure is indeed of vibronic origin, a detailed analysis is required in order to separate the bleaching signal, and a possible contribution to the fine structure, from an electroabsorption signal.

Under certain conditions, two different contributions to $\Delta T/T$ of differing physical origin may have different phases, and as such, it may be possible to separate the contributions according to their phase. Using the data presented here, this can be most easily done for the spectrum taken in accumulation at 110 K, shown in Fig. 8(a), as this is the spectrum that shows the greatest phase difference between the two components, as shown by the nonzero *Y* component at 1.94 eV.

The result of this separation is shown in Fig. 11, plotted alongside the absorption and surface cell electroabsorption spectra taken at a similar temperature, respectively. As has been shown for the room temperature spectra (Fig. 6), the separated bleaching signal shows a strong vibronic structure that is more structured and slightly redshifted than the absorption spectrum of the polymer. The separated electroabsorption component of the CMS spectrum is slightly different from the electroabsorption signal observed in the surface cell geometry, however, this is probably due to differences in the film deposition techniques for the two experiments resulting in differences in the relative strengths of the features. Similar differences, presumably of similar origin, were also observed in the absorption spectra. It is possible that this was

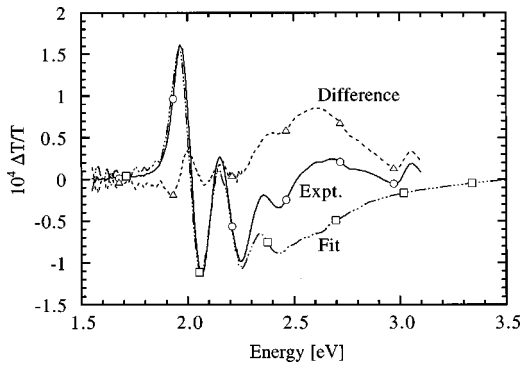

FIG. 12. Electroabsorption of P3HT measured in the surface cell geometry (circles) at room temperature. The fit described in the text is also shown (squares), along with the difference between the two plots (triangles).

due to the fact that the P3HT was deposited by spin coating for the MIS diodes, whereas the polymer was drop cast onto the electroabsorption device structure.

Figure 12 shows the electroabsorption spectrum measured in the surface cell geometry at room temperature. A detailed analysis has been performed by fitting the spectrum to a superposition of the following three contributions:

(1) Zero derivative of absorption* $\Delta f/f$ (representing transfer of oscillator strength to an mA_g exciton).
(2) First derivative of absorption (quadratic stark effect of transition dipole coupling 1 B_u and mA_g).
(3) Second derivative of absorption (linear stark effect due to disorder-induced dipoles).

A good fit is obtained at energies below 2.2 eV. In the region 2.2 to 3.0 eV, the electroabsorption is offset above the derivative fit by a broad feature centered at 2.6 eV, which does not appear in the linear absorption spectrum nor the first or second derivatives. This can be taken as the energy of the dipole-forbidden mA_g exciton, which is normally only seen by two-photon spectroscopy but is partially allowed to an extent $\Delta f/f$ in the presence of an electric field. The much greater linewidth of this feature may in fact be due to a quasicontinuum of closely spaced states in this region; a similarly broad line shape was observed[39] for the methyl-substituted ladder-type polyphenylene, although the inhomogeneous broadening inferred from the linewidth of the 1 B_u exciton is only 30 meV.

The 0-0 origin of the 1 Bu exciton (taken as the zero crossing of the first electroabsorption peak) is at 2.02 eV. The difference in energy between 1 Bu and mAg is therefore 0.59 eV. Considering an isotropic distribution of chain segments, transition dipoles μ and disorder-induced dipoles m,[35,40,41] we can calculate from the quadratic stark effect a transition dipole moment μ of 9.91 eÅ coupling 1 B_u and mA_g. This value of μ implies a transfer of oscillator strength $\Delta f/f$ of 1.4×10^{-4} from 1 B_u to mA_g, (i.e., from one-photon allowed 1 B_u exciton to the one-photon forbidden mA_g exciton), which is also consistent with the area under the broad spectral feature at ca. 2.6 eV. We can also calculate a polarizability of the 1 B_u exciton of 2400 $Å^3$ in cgs units. The

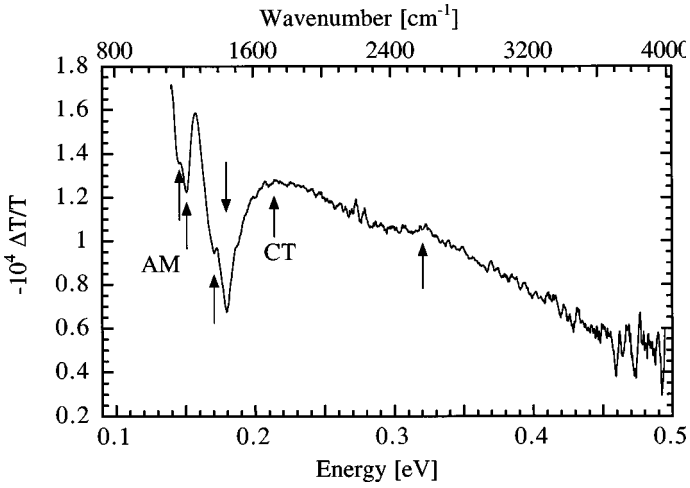

FIG. 13. The CMS spectrum of P3HT measured on a Si wafer FET device in the mid-infrared spectral range. Spectrum taken at room temperature with $V_{on} = -30$ V and $V_{off} = +5$ V.

disorder-induced dipole moment *m* calculated from the linear Stark effect contribution, has a magnitude of 3.16 eÅ.

In order to obtain the full spectroscopic signature of the charge carriers in P3HT FET's, the CMS experiments were also performed in the midinfrared spectral range, the results of which are shown in Fig. 13. Several spectral features of different physical origin are apparent.

The charge-induced absorption increases continuously from 0.5–0.15 eV. This is due to low-energy electronic charge-induced transitions (CT) peaking at energies below the spectral cutoff of our CMS experiments (that is limited by strong infrared absorption in the SiO_2 gate insulator). Recent experiments of photoinduced absorption on thin P3HT films have shown that the peak energy of these transitions is as low as 60 meV.[42] In this broad continuum, we observe a reproducible shoulder at 0.32 eV. It was found that the low-energy electronic transitions below 0.3 eV are more intense the higher the regio-regularity of the polymer and the higher the charge-carrier mobility.[4] In low-mobility, less regio-regular samples, the CMS signal below 0.3 eV is comparatively weak, and a clearly defined peak around 0.35 eV is observed. It is believed that the latter is of the same physical origin as the shoulder seen at 0.32 eV in the high-mobility samples. However, the intense low-energy electronic transitions (CT) below 0.3 eV appear to be characteristic of high-mobility samples. It is possible that they are due to charge-transferlike transitions between neighboring charged and neutral molecules. Such transitions may become intense in high-mobility polymers with strong interchain interactions. Note that the electronic transitions in the midinfrared reported here occur at significantly lower energies than previously reported for more disordered P3HT, in which the lowest-energy transitions of the polarons are observed at energies of 0.4–0.6 eV.[28] This is believed to reflect a reduced relaxation energy in high-mobility, regio-regular P3HT.

Below 0.2 eV, a series of sharp dips in the charge-induced absorption are observed. These are attributed to vibrational modes overlapping with the broad electronic transitions. Reproducible dips are observed at 1216, 1375, and 1448 cm^{-1}.

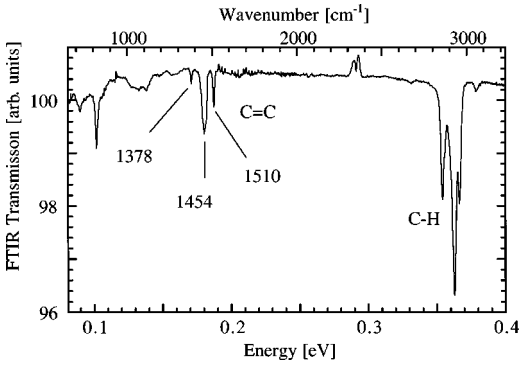

FIG. 14. FTIR absorption spectrum of a thin film of P3HT on a KBr substrate.

These are caused by vibrational modes and/or so-called amplitude modes[43] overlapping with the broad continuum of electronic transitions. Amplitude modes are due to oscillations of the center of mass of the polaronic charge carriers along the polymer chain. Similar observations have been made in photo-induced absorption experiments on P3HT.[42] In the photoinduced absorption experiments covering the full spectral range down to 50 meV, a large number of these sharp antiresonances were observed below 0.12 eV. The appearance of these charge-induced vibrational modes is different from that in low-mobility P3HT in which the electronic transitions at higher energies are not overlapping with the vibrational modes. In this case, only a small number of amplitude modes are observed as distinct sharp peaks.

It was found that the sharp dips in the CMS spectrum of high-mobility P3HT were more pronounced the stronger the low-energy electronic absorption below 0.3 eV, i.e., the higher the regio-regularity and mobility of the polymer.[4] We attribute the sharp dips to a Fano-type antiresonance effect[44] due to the overlap of the continuum of electronic transitions with the charge-induced amplitude modes and/or the symmetric and asymmetric C═C vibrations of the neutral polymer.[4] The latter are observed in the normal thin-film FTIR absorption spectrum (see Fig. 14) close to the dip at 1448 cm^{-1} in the CMS spectrum.[45]

For the charge-induced features present in the CMS spectra in the visible/near-IR spectral range shown in Fig. 5 at 1.34 and 1.65 eV, an estimate of the corresponding transition strengths has been obtained by fitting the spectrum to a superposition of two Gaussian contributions. The area under the curves was calculated to be 1.1×10^{-5} and 7.3×10^{-5} eV, respectively. Although it was not possible to perform the same analysis on the features observed in the mid-IR spectrum due to the overlap between the different transitions, it is reasonable to assume that the feature observed at 0.32 eV is approximately of the same strength as that observed at 1.34 eV because the peak intensities are similar.

The optical absorption cross-sections can also be calculated for the charge-induced subgap transitions observed in the accumulation regime from the equation

$$\frac{\Delta T}{T} = -C\frac{\sigma}{eA}\Delta V$$

where C is the capacitance of the insulator, e is the electronic charge, A is the area of the device, ΔV is the peak-peak amplitude of the ac modulating bias, and σ is the optical cross section of the transition. From the spectrum shown in Fig. 5, the optical cross sections were calculated to be ca. $4.3\times10^{-16}\,\mathrm{cm}^2$ for the feature at 1.34 eV and $6.1\times10^{-16}\,\mathrm{cm}^2$ for the feature at 1.65 eV.

IV. DISCUSSION

The main features of our CMS spectra are as follows:

(1) The charged features are characterized by three subgap optical transitions at 0.32, 1.34, and 1.65–1.74 eV. The peak values of $\Delta T/T$ for the higher-energy transitions observed with CMS for devices biased into accumulation are ca. -0.96×10^{-4} and -3.15×10^{-4}, respectively. The relative oscillator strengths for these two features, in comparison to the feature at ca. 1.34 eV is approximately 1:4 to 1:7, depending upon device preparation. The optical cross sections were calculated to be $4.3\times10^{-16}\,\mathrm{cm}^2$ and $6.1\times10^{-16}\,\mathrm{cm}^2$ at 1.34 and 1.65 eV, respectively, for the spectrum shown in Fig. 5.

(2) The subgap features attributed to charged features are independent of applied bias, modulation frequency, and temperature. This suggests that there is only one charged species present in high-mobility, regioregular P3HT.

(3) A charge transfer (CT) transition is observed at energies below 0.3 eV.

(4) Pronounced vibronic structure is observed in the bleaching signal, but this is absent from the charged features.

(5) An electroabsorption signal is detected when the screening of the injected mobile charge is reduced. This occurs at low temperature and low charge density.

These observations show important differences from previous results, in particular the CMS results on nT (Refs. 30, 31) and disordered, low-mobility P3HT:[28]

(1) CMS studies on nT and disordered P3HT show that an equilibrium exists between singly and doubly charged species, as well as interchain species for a given temperature or charge density. For regioregular, high-mobility P3HT, we observe only one charged species.

(2) We attribute the structure in the π-π^* bleaching signal to vibrational modes on the polymer chain at sites where the charged species are formed. To our knowledge, such a pronounced vibrational structure in the bleaching signal has not been previously reported for a conjugated polymer using CMS or chemical doping of thin solid films.[10,11]

The following experimental observations suggest that the charged species in high-mobility P3HT FET's is a singly-charged polaronic carrier, as opposed to a doubly charged bipolaronic species:

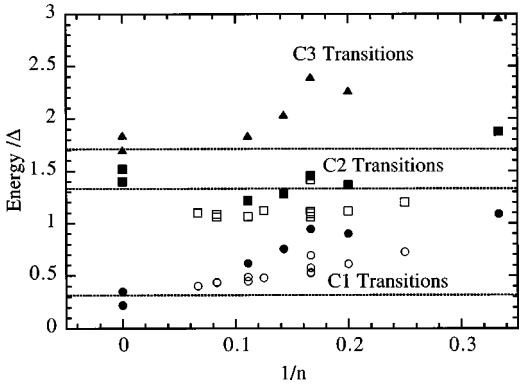

FIG. 15. Summary of polaronic subgap transition energies, normalized to the band gap. Theoretical transitions are shown as solid markers whereas experimental transitions are open markers. Transition $C1$ is depicted by circles, $C2$ by squares, and $C3/4$ by diamonds. See text for a list of references. The three horizontal lines denote the transitions presented here for CMS of P3HT (note that the $C3/4$ transition is equivalent to 1.74 eV).

(1) Bipolarons are expected to be less stable at higher temperature and low charge-carrier concentrations due to entropy considerations.[46,47] If the CMS features were due to bipolaronic carriers, one would therefore expect the spectra to exhibit temperature dependence with bipolaronic species becoming more dominant at low temperatures. This dependence is not observed in the experimental spectra.

(2) We observe three transitions for the charge carrier present in our device and, according to the theoretical models described above, a bipolaron is expected to exhibit a maximum of two transitions (see Fig. 2).

Figure 15 is a composite chart of the experimentally determined and theoretically calculated charge-induced transitions of singly charged radical cationic species in well defined nT^+ and selected polymers. It has been established that an empirical linear relationship exists between the energy of the subgap energy levels and the reciprocal chain length of the oligomer.[8,9,19] In Fig. 15, we plot the energies normalized to half the energy gap, Δ, against $1/n$, with $1/n=0$ corresponding to the idealized limit of an infinite polymer chain. The experimental data on nT^+ is obtained from CMS[28,31] and from chemical doping experiments in solution,[9,48,49] whereas the low-mobility P3HT is obtained from CMS.[28] The theoretically calculated transitions are for polarons in polyacetylene calculated from the FBC model[21] and for nT^+ from quantum chemical calculations.[16–19] The three dotted horizontal lines in Fig. 15 denote the transitions observed in high-mobility P3HT reported here. A comparison shows that whereas the transitions at 0.32 and ca. 1.34 eV may correspond to the $C1$ and $C2$ transitions of nT^+ extrapolated to an effective conjugation length corresponding to that of the polymer, the transition at 1.65–1.74 eV has no analog in the nT^+ charge-induced optical spectra other than for the very weak $C3/4$ transition that is not observed in chemical doping experiments. We discount the possibility of the transition at 1.65–1.74 eV being a vibronic replica of the transition at ca. 1.34 eV as the difference in energy (ca. 0.3–0.4 eV) is too large for vibronic coupling.

TABLE I. Comparison of optical transition strengths between theory and this work, normalized to the strength of the $C2$ transition.

Material	Technique	$\|C1\|$	$\|C2\|$	$\|C3\|$	Reference
$3T$	INDO/SCI	1.25	1.0	0	16
$5T$	INDO/SCI	1.1	1.0	0	16
$6T$	INDO/SCI	1.1	1.0	0	17
$7T$	INDO/SCI	1.1	1.0	0	16
$9T$	INDO/SCI	1.1	1.0	0	16
Trans PA	FBC model	0.9	1.0	$\ll 0.1$	21
Trans PA	Blackman	1.1	1.0	1.9	50
P3HT	CMS	~ 1	1	~ 4–7	This work

Referring to Fig. 2, quantum chemical calculations performed on nT by Cornil *et al.*[16–19] on isolated, one-dimensional chains using Hartree-Fock intermediate neglect of differential overlap with single configuration interactions (INDO SCI) techniques describe why some of the charge-induced, subgap transitions are strong ($C1$, $C2$, and $DC1$) whereas others are either very weak or forbidden ($C3$, $C4$, and $DC2$). Odd numbered oligomers have a C_{2v} symmetry and transitions $C1$, $C2$, and $DC1$ are polarized along the long axis of the molecule, whereas transitions $C3$, $C4$, and $DC2$ are polarized perpendicular to this direction. This results in a far weaker intensity for the latter transitions. For even numbered oligomers, this constraint is even stronger. Here, the molecule has a C_{2h} symmetry and the $C3$, $C4$, and $DC2$ transitions become completely forbidden as states of progressively higher energy have an alternating symmetry between the symmetric b_g and the antisymmetric a_u orbitals.

Interchain interactions have been found to be responsible for the high mobilities in P3HT.[4] As discussed in the introduction, disorder tends to suppress the effects of interchain interactions, however the ordered regions of self-organised P3HT may provide a suitable environment for polaronic carriers to lose their one-dimensional nature.

A study on the effect of interchain coupling on the nature of polaronic charge carriers was done by Blackman and Sabra.[50] Their model was a numerical study based on the SSH model of polyacetylene and built on work by Baeriswyl and Maki.[25] They calculated transition strengths and energies for both polarons and bipolarons in trans-polyacetylene for a range of interchain coupling strengths. When the coupling was negligible, they demonstrated that their results agreed with the FBC model. However, as the interchain coupling increases in strength, the initially very weak transitions of P3 and P4 become intense. For an intermediate interchain coupling regime, the calculated absorption spectrum for a polaron shows three transitions with relative oscillator strengths of 1.1:1.0:1.9 in order of increasing energy. The calculated transition energies are also presented in Fig. 15 where they can be seen to correspond well with the observed features for P3HT.

Table I summarizes the oscillator strengths calculated from the FBC, quantum chemical and Blackman and Sabra models, and the CMS charge-induced features for P3HT presented here for the different singly charged optical transitions. The table shows that the theoretical calculations predict that radical cations should give rise to two optical subgab transitions of roughly equal intensity. The data shown corresponds closely with the experimental spectra of nT^+ and correlates well with the absence of a $C3/4$ transition in the experimental spectra of nT and PT. The observation of one dominant feature at 1.65–1.74 eV with two less, but approximately equally, intense features at lower energies in the CMS spectra presented here is not consistent with these models.

These calculations suggest that the strong transition at 1.65–1.75 eV may be related to the $C3$ transition of the isolated chain models with its intensity reflecting the strength of interchain interactions as modeled by Blackman and Sabra. This reveals the two-dimensional nature of the polaronic charge carriers brought about by interchain interactions coupled to the high intra- and inter-chain order in the polymer. The charge carrier wave functions are no longer confined to a single chain, but are spread over neighboring chains.[23]

The Blackman and Sabra calculations are based on a very simple model of polyacetylene and neglect electron-electron interactions. For a full theoretical understanding of the CMS spectra, a proper treatment of interchain and electron-electron interactions will be required. Quantum mechanical calculations on interchain coupled oligothiophene molecules may provide more insight into the effects of interchain coupling.[51]

It should be noted that Ziemelis also attributed a weak feature observed at 2.16 eV to the $C3/4$ transition in regio-random P3HT. The weak intensity of this transition may reflect the higher degree of disorder of the regio-random P3HT used in this experiments. Disorder would limit the ability of polarons to exhibit a quasi-two-dimensional nature and, hence, reduce the intensity of the $C3/4$ transition.

The presence of a CT transition at energies below ca. 0.3 eV may also be taken as further evidence for the strong interchain interactions present in P3HT. As discussed above, in the case of isolated chains, no electronic transitions are observed below the energy of the $C1$ transition. Below $C1$, there are only a small number of charge vibrational modes that appear as sharp peaks in photo-induced absorption spectra.[12] We believe that the low-energy electronic transitions in regio-regular P3HT overlapping with vibrational modes, which make the latter appear as antiresonances, is also a manifestation of the pronounced degree of interchain interaction. We expect that were it possible to further enhance the interchain packing, the CT transition would evolve into a Drude-like intraband absorption response. Similar charge-transfer features are typically observed for well ordered π-stacked molecules[52] and the presence of such a feature in the spectra presented here can be taken as further evidence for the possible 2D nature of the wave function of the charge carriers present in high-mobility P3HT.

As we have discussed above, the high intensity of the $C3/4$ transition relative to the $C1$ and $C2$ transitions and the high resolution of the vibronic structure in the bleaching of the π-π^* absorption is indicative of the high degree of order of the sites where the charge carriers reside. Close analysis of the dc bias dependent CMS spectra shown in Fig. 9 reveal

small, repeatable differences between the spectra taken in accumulation at 0 and −5 V that suggest the spectrum taken at 0 V probes sites that exhibit slightly greater order than those probed at −5 V. Compared to the spectrum taken at 0 V, the spectrum taken at −5 V exhibits a bleaching signal that is slightly less well-resolved, a $C2$ transition of slightly greater intensity by a factor of ca. 1.05 and a slightly redshifted $C3/C4$ transition by ca. 0.01 eV. This effect is due to the difference between the charge density in the accumulation layer at 0 V and −5 V. These results suggest that the states probed at −5 V are occupied by charge carriers that are slightly less two-dimensional in character to those probed at 0 V and, hence, that the charges occupy sites with slightly greater associated disorder. Charge injected into the polymer rapidly relaxes to the unoccupied state of lowest energy such that as the amount of charge stored in the polymer increases states of higher energy that are gradually filled. These results are therefore consistent with sites of higher energy being associated with a higher degree of disorder.

We note that Mizes and Conwell[53] investigated the interchain stability of polarons in poly(phenylenevinylene) (PPV) in a system of two defect free interacting oligomers composed of four repeat units, each oriented in a herringbone crystal structure. They concluded that in PPV, polarons are stabilized on a single chain. P3HT, however, exhibits a lamella structure with strong cofacial π-π interchain stacking and this difference highlights how sensitive the interchain character of polaronic charge carriers may be to the nature of the solid-state packing of the polymer chains.

Figures 6 and 11 show that the vibronic structure in the bleaching signal is both sharper and slightly redshifted above 2.0 eV with respect to the absorption spectrum. This suggests that the charge carriers form on chain segments that exhibit greater structural order than the complete set of chains participating in total absorption of light. This suggests that charge carriers reside only on the most ordered chain segments.

The lack of corresponding vibronic structure in the charge features is intriguing. Note that for isolated chains of nT in solution, vibrational structure in the charged-induced features has been observed during chemical doping experiments.[6,9] The absence of vibronic structure in the charged transitions of P3HT cannot be attributed to inhomogeneous broadening due to intrachain disorder since the corresponding bleaching signal exhibits a pronounced vibronic structure. It is possible that the lack of vibronic structure in the charged features reflects a sensitive dependence of the characteristics of the two-dimensional polaronic charge carriers on the strength of the interchain coupling, such that the charged transitions may be easily broadened by interchain disorder. This dependence may be more pronounced than for the neutral excitation bleached by the presence of the charge carrier. An alternative explanation may be that the lack of vibrational structure is an intrinsic manifestation of the two-dimensional nature of the charge carriers, reflecting, for example, a reduced coupling to intramolecular vibrations. This is an open question that may warrant detailed theoretical investigations.

V. CONCLUSION

Regio-regular P3HT is a polymer with several remarkable properties. Due to its high level of intrachain order, the polymer self-assembles into regions of high-interchain order and this has the effect of increasing the field-effect mobility of injected charge carriers by two to three orders of magnitude to ca. 0.1 cm^2/Vs, compared to regio-random P3HT. The CMS experiments reported here have shown that the high degree of interchain order changes the nature of the charge carriers. Only one singly charged species is observed, independent of charge density and temperature, which suggests that the intrinsic charge carrier of P3HT is being detected. Furthermore, it has been shown that this charge carrier has properties that are significantly different from those observed for isolated 1D polymer chains. The presence of a strong charge-induced, subgap feature at energies close to the π-π^* transition and low-energy CT transitions reflects a reduced degree of polaronic relaxation and suggests that the charge carriers have taken on a 2D, interchain characteristic. It may be possible that given the strength of this transition and a suitable theoretical framework, an estimate of the strength of the interchain interaction may be obtained.

ACKNOWLEDGMENTS

We acknowledge A. Flewitt for preparing the SiO_2 gate insulator by PECVD. This work was supported by the European Commission (ESPRIT 24793-FREQUENT). P.J.B. would like to thank the Engineering and Physical Sciences Research Council and Philips Research Laboratories, Eindhoven, for financial support.

*Corresponding author. Email: hs220@phy.cam.ac.uk Fax: +44 (0)1223 353397

[1] Z. Bao, A. Dodabalapur, and A. J. Lovinger, Appl. Phys. Lett. **69**, 4108 (1996).

[2] H. Sirringhaus, N. Tessler, and R. H. Friend, Science **280**, 1741 (1998).

[3] T. A. Chen, X. M. Wu, and R. D. Rieke, J. Am. Chem. Soc. **117**, 233 (1995).

[4] H. Sirringhaus, P. J. Brown, R. H. Friend, M. M. Nielsen, K. Bechgaard, B. M. W. Langeveld-Voss, A. J. H. Spiering, R. A. J. Janssen, E. W. Meijer, P. Herwig, and D. M. de Leeuw, Nature (London) **401**, 685 (1999).

[5] A. Assadi, C. Svensson, M. Willander, and O. Inganas, Appl. Phys. Lett. **53**, 195 (1988).

[6] D. Fichou, G. Horowitz, B. Xu, and F. Garnier, Synth. Met. **1990**, 243 (1990).

[7] D. Fichou, G. Horowitz, and F. Garnier, Synth. Met. **1990**, 125 (1990).

[8] G. Horowitz, A. Yassar, and H. J. von Bardeleben, Synth. Met. **62**, 245 (1994).

[9] J. A. E. H. van Haare, E. E. Havinga, J. L. J. van Dongen, R. A. J. Janssen, J. Cornil, and J. L. Bredas, Chem.-Eur. J. **4**, 1509 (1998).

[10] T. C. Chung, J. H. Kaufman, A. J. Heeger, and F. Wudl, Phys.

Rev. B **30**, 702 (1984).
[11] K. Kaneto, S. Hayashi, S. Ura, and K. Yoshino, J. Phys. Soc. Jpn. **54**, 1146 (1985).
[12] Z. Vardeny, E. Ehrenfreund, O. Brafman, M. Nowak, H. Schaffer, A. J. Heeger, and F. Wudl, Phys. Rev. Lett. **56**, 671 (1986).
[13] P. A. Lane, X. Wei, Z. V. Vardeny, J. Poplawski, E. Ehrenfreund, M. Ibrahim, and A. J. Frank, Synth. Met. **76**, 57 (1996).
[14] P. A. Lane, X. Wei, and Z. V. Vardeny, Phys. Rev. Lett. **77**, 1544 (1996).
[15] Y. Furukawa, J. Phys. Chem. **100**, 15 644 (1996).
[16] J. Cornil, D. Beljonne, and J. L. Bredas, in *Electronic Materials: The Oligomer Approach*, 1st ed., edited by K. Mullen and G. Wegner (Wiley-VCH, Weinheim, 1998), pp. 432–447.
[17] J. Cornil, D. Beljonne, V. Parente, R. Lazzaroni, and J. L. Bredas, in *Handbook of Oligo- and Polythiophenes*, 1st ed., edited by D. Fichou (Wiley-VCH, Weinheim, 1999), pp. 317–339.
[18] J. Cornil, D. Beljonne, and J. L. Bredas, J. Chem. Phys. **103**, 834 (1995).
[19] J. Cornil, D. Beljonne, and J. L. Bredas, J. Chem. Phys. **103**, 842 (1995).
[20] W. P. Su, J. R. Schrieffer, and A. J. Heeger, Phys. Rev. Lett. **42**, 1698 (1979).
[21] K. Fesser, A. R. Bishop, and D. K. Campbell, Phys. Rev. B **27**, 4804 (1983).
[22] M. Deussen and H. Bassler, Synth. Met. **54**, 49 (1993).
[23] D. Emin, Phys. Rev. B **33**, 3973 (1986).
[24] D. Emin and M. N. Bussac, Phys. Rev. B **49**, 14 290 (1994).
[25] D. Baeriswyl and K. Maki, Synth. Met. **28**, D507 (1989).
[26] H. A. Mizes and E. M. Conwell, Phys. Rev. Lett. **70**, 1505 (1993).
[27] Y. Furukawa, N. Yokonuma, M. Tasumi, M. Kuroda, and J. Nakayama, Mol. Cryst. Liq. Cryst. Sci. Technol., Sect. A **256**, 113 (1994).
[28] K. E. Ziemelis, A. T. Hussain, D. D. C. Bradley, R. H. Friend, J. Ruhe, and G. Wegner, Phys. Rev. Lett. **66**, 2231 (1991).
[29] M. G. Harrison, R. H. Friend, F. Garnier, and A. Yassar, Mol. Cryst. Liq. Cryst. Sci. Technol., Sect. A **252**, 165 (1994).
[30] M. G. Harrison, R. H. Friend, F. Garnier, and A. Yassar, Synth. Met. **67**, 215 (1994).
[31] M. G. Harrison, D. Fichou, F. Garnier, and A. Yassar, Opt. Mater. **9**, 53 (1998).
[32] S. M. Sze, *Physics of Semiconductor Devices*, 2nd ed. (Wiley, Chichester, 1981).
[33] E. J. Samuelsen and J. Mardalen, in *Handbook of Organic Conductive Polymers; Vol. 3. Conductive Polymers: Spectroscopy and Physical Properties*, 1st ed., edited by H. S. Nalwa (Wiley, Weinheim, 1997), pp. 100–106.
[34] M. Cardona, *Modulation Spectroscopy*, Vol. 11, 1st ed. (Academic, London, 1969).
[35] A. Horvath, G. Weiser, G. L. Baker, and S. Etemad, Phys. Rev. B **51**, 2751 (1995).
[36] H. Sirringhaus, N. Tessler, and R. H. Friend, Synth. Met. **102**, 857 (1999).
[37] A. R. Brown, C. P. Jarrett, D. M. de Leeuw, and M. Matters, Synth. Met. **88**, 37 (1997).
[38] M. G. Harrison, J. Gruner, and G. C. W. Spencer, Synth. Met. **76**, 71 (1996).
[39] M. G. Harrison, S. Moller, G. Weiser, G. Urbasch, R. F. Mahrt, H. Bassler, and U. Scherf, Phys. Rev. B **60**, 8650 (1999).
[40] A. Horvath, H. Bässler, and G. Weiser, Phys. Status Solidi B **173**, 755 (1992).
[41] G. Weiser and A. Horvath, Chem. Phys. **227**, 153 (1998).
[42] R. Osterbacka, C. P. An, X. M. Jiang, and Z. V. Vardeny, Science **287**, 839 (2000).
[43] B. Horowitz, Solid State Commun. **41**, 729 (1982).
[44] U. Fano, Phys. Rev. **124**, 1866 (1961).
[45] Y. Furukawa, M. Akimoto, and I. Harada, Synth. Met. **18**, 151 (1987).
[46] M. J. Nowak, D. Spiegel, S. Hotta, A. J. Heeger, and P. A. Pincus, Macromolecules **22**, 2917 (1989).
[47] M. J. Nowak, D. Spiegel, S. Hotta, A. J. Heeger, and P. A. Pincus, Synth. Met. **28**, C399 (1989).
[48] D. Fichou, G. Horowitz, B. Xu, and F. Garnier, Synth. Met. **39**, 243 (1990).
[49] M. A. Sato and M. Hiroi, Polymer **37**, 1685 (1996).
[50] J. A. Blackman and M. K. Sabra, Phys. Rev. B **47**, 15 437 (1993).
[51] D. Beljonne (unpublished).
[52] D. D. Graf, R. G. Duan, J. P. Campbell, L. L. Miller, and K. R. Mann, J. Am. Chem. Soc. **119**, 5888 (1997).
[53] H. A. Mizes and E. M. Conwell, Synth. Met. **68**, 145 (1994).